Journal of Lasers, Optics & Photonics
ISSN: 2469-410X

Lotscher et al., J Laser Opt Photonics 2015, 2:3
DOI: 10.4172/2469-410X.1000124

Research Article Open Access

Long-term Stability of Nonlinear Pulse Compression using Solid-core Large-mode-area Fibers

Lauryna Lotscher[1,2*], **Lenard Vamos**[2], **Laszlo Veisz**[1] **and Alexander Apolonski**[1,2]

[1]*Max-Planck-Institute of Quantum Optics, Hans-Kopfermann-Str. 1, 85748 Garching, Germany*

[2]*Ludwig Maximilian University of Munich, Am Coulombwall 1, 85748 Garching, Germany*

[*]**Corresponding author:** Lauryna Lotscher, Max-Planck-Institute of Quantum Optics, Hans-Kopfermann-Str. 1, 85748 Garching, Germany, Tel: +4915-7733-12373; E-mail: lauryna.loetscher@mpq.mpg.de

Received date: Sep 17, 2015; **Accepted date:** Nov 19, 2015; **Published date:** Nov 25, 2015

Abstract

Long-term stability of a laser system is crucially important for applications such as ultrafast laser spectroscopy. Unfortunately, this topic received little attention in novel pulse compression schemes. Through the ultra-stable beam pointing of the 50 kHz laser system, the long-term stability of nonlinear pulse compression (NPC) was measured for up to 17 hours at different peak powers in a fiber core. The required spectral broadening was achieved in large-mode-area photonic-crystal-fibers with linearly and circularly polarized light. The optimal parameters of a NPC system operating close to the fundamental limit of the critical self-focusing peak power were found. A further compression to sub-10 fs pulses in a second fiber stage is also discussed.

Keywords: Nonlinear pulse compression; Regenerative amplifier; Photonic crystal fiber; Self-phase modulation; Kerr-effect

Introduction

Nonlinear pulse compression (NPC) is a well-known technique. In a first step, the optical and width is increased, typically with a nonlinear interaction such as self-phase modulation (SPM). Thereafter, the pulse duration is strongly reduced by a linear dispersive compressor. By NPC the shortest light pulses were generated approaching the fundamental limit of a single wave cycle using different spectral broadening platforms (bulk, solid-core and gas-filled waveguides) depending on laser input parameters [1-5], which enabled new experiments and a new field of physics, the attosecond science [6]. Ytterbium lasers in combination with NPC provide ultrashort pulses at increasingly higher repetition rates and pulse energies [5,7-14]. However, the main open question is the long-term stability of NPC, especially when operating close to the fundamental limit of the critical self-focusing peak power.

We have performed the long-term stability measurements of NPC with the spectral broadening in solid-core large mode area (LMA) photonic-crystal-fibers (PCF), because such a setup is simple and can be easily implemented into a more complex laser system required for different ultra-short applications. One example is an electron pulse characterization by a streaking of electron pulses in infrared or terahertz fields [15]. For terahertz pulse generation, picosecond pulses emitted by Yb: YAG amplifiers are optimal [16,17], however significantly shorter electron pulses and thus shorter pulses of a laser field are preferred in the experiment. Another example is high-power Yb-frontend optical parametric chirped pulse amplifiers (OPCPA). The pulse duration of 1 ps is optimal to pump an ultra-short OPCPA [18]. A broadband seed, however, should be generated from a narrowband Ytterbium amplifier output. It is well known, that shorter pulses have clear advantages for generating powerful and stable white-light super continuum [19-24].

Materials and Methods

The theory behind SPM is well known. spectral broadening can be calculated according to equation 1 [25]:

$$S(\omega) = |\tilde{U}(L,\omega)|^2,$$

$$= |F\{U(,)e^{i\phi NL(L,T)}\}|^2$$

where S (ω) is the output spectrum, *U(0; T)* is the input field amplitude, L is the fiber length, *T* is the time with respect to a frame of reference travelling at the group velocity of the pulse, and (L; T) is the nonlinear phase as induced by self-phase modulation [25]:

$$\phi_{NL}(L,T) = |\tilde{U}(0,T)|^2 \gamma P_0 L,$$

Where γ is the nonlinear parameter and P0 is the peak power. The fundamental limit of the technique is given by the critical self-focusing peak power of fused-silica: 4 MW for linear and 6 MW for circular polarization [11,26,27]. In this paper we investigated in detail the dependence of the long-term stability on the peak power when operating close to the critical self-focusing peak power in the fiber core. After the spectral broadening, the pulse duration is strongly reduced by a linear dispersive compressor. We calculated the group delay dispersion (GDD) of a linear dispersion compressor by summing up the GDD of the fiber material and the GDD due to SPM similar to [28]:

$$GDD_{SPM} = \frac{\lambda \cdot \tau_0^2}{16 \cdot ln(2) \cdot \pi \cdot L \cdot n_2 \cdot I_0},$$

Where λ is the central wavelength of the laser; τ_0 - the pulse duration (FWHM); *L* - the fiber length; n_2 - the nonlinear refractive index of a silica-core fiber (no dopants inside the core) 2:36 × 1016 cm^2/W [29]; I_0 - the peak intensity of a laser pulse for the mode area at $1/e^2$ level. An assumption was made that only the temporal phase changes during the propagation, whereas the temporal intensity stays the same. This is valid because of long input pulses. The experiment

was driven by an Yb:YAG regenerative amplifier [30]. The experimental setup is shown in Figure 1a. A repetition rate of the laser was adjustable from 50 kHz to 300 kHz with the measured 1.1 ps and 0.8 ps pulse duration, respectively. An introduced chirp before the amplifier was compensated by a grating compressor optimized at 300 kHz repetition rate. The dependence of the pulse duration on the repetition rate was not investigated in details. Presumably, it can be explained by thermal changes of air-cooled transmission gratings of the compressor operating at high average power. For the NPC experiments, 50 kHz was chosen, because of forthcoming electron diffraction experiments. Such a compromised repetition rate reduces thermal effects of thin films under study while allowing to collect enough data during an hour-scale period.

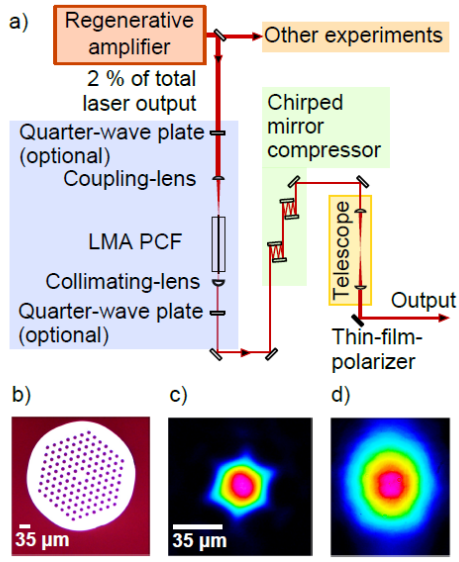

Figure 1: (a) NPC setup. Lasers: Yb:YAG thin-disk regenerative amplifier (20 W at 50 kHz, pulse duration 1 ps, beam diameter 38 mm at $1/e^2$ level), coupling-lens (focal length 75 mm), fiber. NKT Photonics LMA-35 fiber, collimating lens (focal length 18 mm), chirped mirror compressor (22 reflection, average value of GDD -540 fs^2/reflection in the spectral range from 980 nm to 1060 nm), (b) Fiber cross-section, (c) Coupled mode in near-field, (d) coupled mode in far-field.

A small part of the amplifier output (maximally 2%, 400 mW, due to the critical self-focusing limit of a fiber) was focused into a LMA PCF (LMA-35, NKT Photonics, and Denmark). The rest of the power was used for experiments described in [30]. To match the mode of the fiber the required focal length and the numerical aperture of the coupling lens were calculated using the ABCD matrix. The complex q parameter of the laser beam was evaluated by measuring the beam diameter (at $1/e^2$ level) with a beam profiling camera within a certain distance (Figure 1b). The laser beam (38 mm in diameter at $1/e^2$ level) was coupled into the fiber by a 75 mm Plano-convex lens. The end-facet of the fiber was imaged by another lens (achromatic, focal length ≈ 18.4 mm) on the beam profiling camera to optimize the coupling. In order to avoid birefringence in the fiber due to stress induced by mounting, the fiber was freely lying in a V-groove mount fixed on a xyz translation stage (NanoMax, Thorlabs, USA). Commercially available solid core LMA fibers are limited to a mode field diameter (MFD) of 26 µm (LMA-35 fibers [31]), defining thus our choice of the fiber and the range of pulse energies. The near-field image of the coupled light in the fiber core is shown in Figure 1c. The coupling monitored by the near-field imaging was stable within days because of an implemented integrated active beam stabilization system (Aligna, TEM Messtechnik, Germany). Also, thermal drifts can be excluded in our experiments, because the input average power of the laser was low. The coupling efficiency into the fiber core was 77%. We calculated this number as the ratio of the power, when the cladding modes where blocked by a pinhole placed at the near-field image of the fiber end-facet, and the total output power. The result agreed well with the additional measurement in the far-field without a pinhole, when the cladding-modes were blocked by the optical mounts. A quarter-wave plate placed before the coupling lens was used as an optional element in the setup for transforming the polarization from linear to circular. The polarization was transformed back by another quarter-wave plate after the collimating lens. Pulses were compressed with a chirped mirror compressor with -540 fs^2 GDD per reflection in the spectral range from 980 nm to 1060 nm.

The aim of the experiment was to generate as short as possible pulses of highest pulse energy, with its stable operation for several hours. We started with a short 35 mm piece of the fiber, because in general, the shorter the fiber, the higher pulse energy can be coupled in order to realize the same transform-limited pulse duration corresponding to the output spectrum. Below in the text, we used the value of a transform-limited pulse duration to characterize broadened spectra resulted from SPM. For the long-term stability characterization, the input power reference, the output power and the spectra were simultaneously measured. We conducted long-term stability measurements with increasingly longer fiber pieces and thus lower pulse energies necessary for producing the same spectral bandwidth, in order to find the optimal conditions. Some minor fluctuations within 2 minute period were visible as the result of a laser cooling system [30]. A home-made second harmonic generation frequency resolved optical gating (SHG FROG) device was used to characterize compressed pulses.

Results and Discussion

Experimentally we reached the critical self-focusing peak power both with linear and circular polarization with a 35 mm fiber piece. To the best of our knowledge, the critical self-focusing peak power was reached only in fibers of a significantly larger MFD: 60 m [11,32] and 75 m [33]. Numerical simulations show that the peak power close to the critical self-focusing limit can be achieved only in LMA fibers with MFD more than 40 m [27], whereas in fibers of smaller diameter damage occurs due to other fundamental mechanisms occurring at lower values. We have not observed any abrupt fiber damage at critical self-focusing limit but rather output power degradation (Figure 2). The output pulse energy decayed with a significant rate of 8 nJ per minute at slightly lower level (3.4 MW) than the critical self-focusing peak power for linear polarization. As a result, after 75 minutes the output dropped by 15%. Output decay was recorded also with an 80 mm long fiber. The output pulse energy decreased by 3% in the first 60 minutes and stayed almost steady thereafter. However it decreased additionally by 5% in the following 16 hours. With a 100 mm long fiber, no decay was observed both with linear and circular polarizations. The output pulse energy with a 100 mm fiber and circular polarization was as high as with an 80 mm fiber and linear polarization. We have measured the output power daily with a 100 mm fiber and circular polarization and

noticed an almost negligible reversible drop in the output, which is expectable for a common free-space coupling into the fiber.

The pulse-to-pulse stability was additionally measured with a photodiode and an oscilloscope. The pulse-to-pulse stability within a short time span (10 ms) was 1.1% rms for input pulses and 1.2% for the output with a 100 mm long fiber both with linear and circular polarizations.

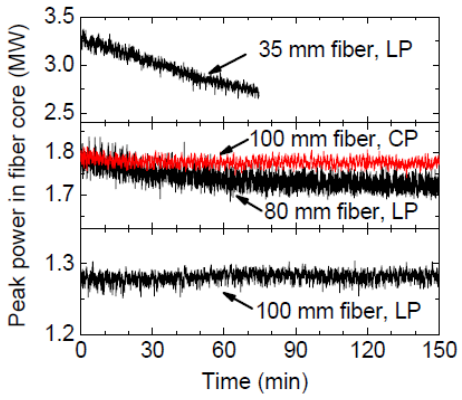

Figure 2: Output pulse energy within 2.5 hours for the same spectral broadening (transform-limited pulse duration: 66 fs), but different fiber lengths: 35 mm, linear polarization (LP); 80 mm, Lp; 100 mm, LP and circular polarization (CP).

The polarization extinction ratio (PER) of the input beam was 31 dB, whereas the output beam continuously degraded with energy, down to 14 dB. The PER of the spectral broadened output is lower than of the input, because SPM also results into a nonlinear polarization rotation [25,34]. The PER was lightly improved by 3 dB with a quarter-wave plate, by rotating the plate 10 degrees. A half-wave plate additionally added a slight improvement of 0.6 dB. For these measurements, we used zero order retardation plates. This observation let us conclude, that not only the nonlinear polarization rotation, but also a depolarization happened in the fiber. No difference in the PER value was measured achieving the same spectral bandwidth with linear and circular polarization in the fiber, because the degradation of the PER depends on the effective electromagnetic field. The PER value of the output (14 dB) was still good enough to use the beam without significant losses.

The validity of the equation 3 was checked firstly for linear laser polarization and 1.5 J pulse energy in the fiber core. The dispersion introduced by SPM was found to be 6066 fs^2. Chromatic dispersion has two parts: 1900 fs^2 in a 100 mm fiber piece and 1620 fs^2 in two non-polarizing beam splitter cubes (N-BK7 glass) mounted in the SHG FROG device, with the sum of the lengths equal to 50 mm. The total calculated dispersion value reached 9586 fs^2. The shortest pulses were measured with 22 bounces. The experimentally found value of the introduced GDD for realizing the shortest pulses was 11880 fs^2, which deviated by 20% from the calculated value. The discrepancy between the measured and the calculated dispersion can be attributed to the accuracy in the GDD value of the chirped mirrors. During the propagation in the fiber, as the spectral bandwidth increases, the input pulse intensity decreases due to the chromatic dispersion. This was not taken into account in the calculations. However, for long (1 ps) input pulses, the GDD due to SPM contributed more than 50% to the total linear compression dispersion. This simple estimation can be used for evaluating the required GDD, making the first compressor design steps significantly easier. As the next step, we have found experimentally that the amount of the necessary GDD for linear and circular polarizations were the same for similar spectral broadening. The reconstructed pulse had duration of 70 fs (FWHM), whereas the transform-limited pulse duration calculated from the measured spectrum was equal to 66 fs. The main peak contained about 57% of the pulse energy. The total compressor efficiency reached 67%, since the reflection per bounce was 98.2%. The total pulse energy was 1.4 J after the compressor and some optics (5 silver mirrors, 2 AR-coated lenses of a telescope, and a thin--polarizer) in a linear s-polarization.

"Red-light" output was observed, when a certain spectral bandwidth was reached (supporting 53 fs). Spectral measurements indicated that not only light in visible, but also additional spectral components in infrared were generated (Figure 3a). Following [35], degenerate four-wave-mixing (DFWM) in the fiber was the reason, because LMA-35 can provide phase matching for signal and idler wavelengths with more than two octaves of separation in the spectrum, since chromatic dispersion of the fiber with such a large core almost equals dispersion of bulk [25]. Additionally, a short fiber length and long input pulses are advantageous for a good overlap of the modes of the interacting waves. A clear indication for DFWM are the peaks at 854 nm and 1251 nm (Figure 3a, blue line), which can be explained by 1015 nm + 1015 nm → 854 nm + 1251 nm. With a 35 mm piece of fiber "red-light" was observed at 4.1 MW peak power for linear and at 5.8 MW peak power for circular polarization, whereas with a 100 mm fiber at 1.9 MW for linear polarization. After about 30 minutes after its appearance, the "red-light" disappeared. The long-term stability measurements indicated the total output degradation (Figure 3b). We also tried a 100 mm fiber with end-caps. For the fiber with the end-caps, "red-light" generation was observed at the same threshold indicating that the process happens in the fiber but not on its facets. Also, the long-term stability was not improved by using the end-caps. The output power degradation observed was similar to the Type I damage of a dielectric material associated with a permanent change of refractive index due to generated electron hole plasma produced by multiphoton band-to-band transitions [36].

The optimal peak power in the fiber core at 50 kHz repetition rate was 1.8 MW using circular polarization. A systematic study of the long-term stability at MHz repetition rate was not reported. Two di_erent regimes of material modification have been identified in writing optical waveguides in glass - the low repetition rate regime (<200 kHz) and the high repetition rate regime (>1 MHz) [37]. In the latter thermal diffusion and cumulative effects is of major importance. We believe that similar regimes can be identified regarding the long-term stability.

In order to reach a spectrum supporting few-cycle pulses, a second fiber stage was considered. However, due to the critical self-focusing peak power only a fraction (30%) of the total output could be used. We considered chirped pulse NPC in the second stage. However, the approach was unsuccessful, because the generated modulated spectral shape leads to a complicated temporal profile of chirped pulses. The same spectral components are generated due to SPM at different time, since the change in refractive index depends on temporal pulse intensity I in the following way: $dn(I)=dt = n_2.dI=dt$. This results in a complicated spectral phase of a SPM spectrum, which is hard to compensate. Even if the input pulses were transforming limited, they would get chirped significantly when propagating in the fiber. An

alternative promising approach for achieving an octave-spanning spectrum and sub-10 fs pulses with 1 ps input pulses is white-light-generation in crystals with compressed sub-100 fs pulses out of the fiber NPC stage.

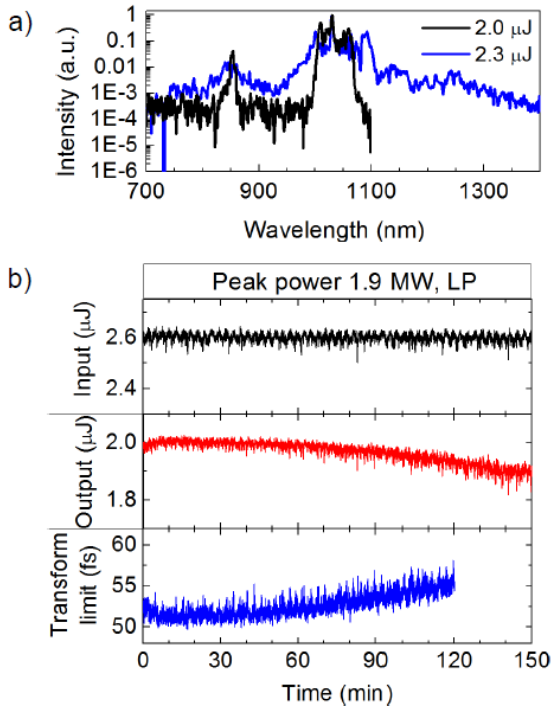

Figure 3: Spectra of SPM and FWM at 2.0 J output and 2.3 J output pulse energy (a) long-term stability at 2.0 j output (b) with a 100 mm fiber.

Conclusion

In conclusion, we demonstrated a long-term stable 70-fs 1.4 J pulses realized with one-stage nonlinear pulse compression of the output of an 1-ps Yb:YAG regenerative amplifier. The optimal peak power in the fiber core was 1.8 MW using circular polarization at 50 kHz repetition rate.

Acknowledgments

We acknowledge funding from the Munich-Centre for Advanced Photonics. We are grateful to Dr. P. Baum for the laser beam time and helpful comments on the manuscript, W. Schneider and R. Graf for helping out with the regenerative amplifier, and Dr. V. Pervak for chirped mirrors. We also acknowledge help from V. Henderson regarding theoretical simulations. Moreover, we are grateful to Dr. N. Karpowicz and M. Seidel for the simulations with a second fiber stage and the helpful tips regarding the SHG FROG retrievals.

References

1. Baltuska A, Wei Z, Pshenichnikov MS, Wiersma DA (1997) Optical pulse compression to 5 fs at a 1-MHz repetition rate. Opt Lett 22: 102-104.
2. Nisoli M, Stagira S, De Silvestri S, Svelto O, Sartania S, et al. (1997) A novel-high energy pulse compression system: generation of multigigawatt sub-5-fs pulses. Appl Phys B 65: 189-196.
3. Heidt AM, Rothhardt J, Hartung A, Bartelt H, Rohwer EG, et al. (2011) High quality sub-two cycle pulses from compression of supercontinuum generated in all-normal dispersion photonic crystal fiber. Opt Express 19: 13873-13879.
4. Demmler S, Rothhardt J, Heidt AM, Hartung A, Rohwer EG, et al. (2011) Generation of high quality, 1.3 cycle pulses by active phase control of an octave spanning supercontinuum. Opt Express 19: 20151-20158.
5. Pronin O, Seidel M, Lucking F, Brons J, Fedulova E, et al. (2015) High-power multi-megahertz source of waveform-stabilized few-cycle light. Nat Commun 6: 1-6.
6. Corkum PB, Krausz F (2007) Attosecond science. Nature Physics 3: 381-387.
7. Sudmeyer T, Brunner F, Innerhofer E, Paschotta R, Furusawa K, et al. (2003) Nonlinear femtosecond pulse compression at high average power levels by use of a large-mode-area holey fiber. Opt Lett 28: 1951-1953.
8. Hadrich S, Rothhardt J, Eidam T, Limpert J, Tunnermann A (2009) High energy ultrashort pulses via hollow fiber compression of a fiber chirped pulse amplification system. Opt Express 17: 3913-3922.
9. Hadrich S, Carstens H, Rothhardt J, Limpert J, Tunnermann A (2011) Multi-gigawatt ultrashort pulses at high repetition rate and average power from two-stage nonlinear compression. Opt Express 19: 7546-7552.
10. Heckl OH, Saraceno CJ, Baer CRE, Sudmeyer T, Wang YY, et al. (2011) Temporal pulse compression in a xenon-filled Kagome-type hollow-core photonic crystal fiber at high average power. Opt Express 19: 19142-19149.
11. Jocher Ch, Eidam T, Hadrich S, Limpert J, Tunnermann A (2011) Sub 25 fs pulses from solid-core nonlinear compression stage at 250 W of average power. Opt Lett 37: 4407-4409.
12. Emaury F, Dutin CF, Saraceno CJ, Trant M, Heckl OH, et al. (2013) Beam delivery and pulse compression to sub-50 fs of a modelocked thin-disk laser in a gas-filled Kagome-type HC-PCF fiber. Opt Express 21: 4986-4994.
13. Hadrich S, Klenke A, Hoffmann A, Eidam T, Gottschall T, et al. (2013) Nonlinear compression to sub-30-fs, 0.5 mJ pulses at 135 W of average power. Opt Lett 38: 3866-3869.
14. Mak KF, Seidel M, Pronin O, Frosz MH, Abdolvand A, et al. (2015) Compressing µJ-level pulses from 250 fs to sub-10 fs at 38-MHz repetition rate using two gas-filled hollow-core photonic crystal fiber stages. Opt Lett 40: 1238-1241.
15. Kirchner FO, Gliserin A, Krausz F, Baum Peter (2014) Laser streaking of free electrons at 25 keV. Nature Photonics 8: 52-57.
16. Hebling J, Yeh KL, Hoffmann MC, Nelson KA (2008) High-power THz generation, THz nonlinear optics, and THz nonlinear spectroscopy. IEEE J. Sel. Topics Quantum Electron 14: 345-353.
17. Hirori H, Tanaka K (2013) Nonlinear optical phenomena induced by intense single-cycle terahertz pulses. IEEE J Sel Topics Quantum Electron 19: 8401110-8401110.
18. Ross IN, Matousek P, New GHC, Osvay K (2002) Analysis and optimization of optical parametric chirped pulse amplification. J Opt Soc Am B 19: 2945-2956.
19. Bradler M, Baum P, Riedle E (2009) Femtosecond continuum generation in bulk laser host materials with sub-µJ pump pulses. Appl Phys B 97: 561-574.
20. Schulz M, Riedel R, Willner A, Mans T, Schnitzler C, et al. (2011) Yb:YAG Innoslab amplifier: effcient high repetition rate subpicosecond pumping system for optical parametric chirped pulse amplification. Opt Lett 36: 2456-2458.
21. Homann Ch, Bradler M, Forster M, Hommelho P, Riedle E (2012) Carrier-envelope phase stable sub-two-cycle pulses tunable around 1.8 µm at 100 kHz. Opt Lett 37: 1673-1675.

22. Riedel R, Schulz M, Prandolini MJ, Hage A, Hoppner H, et al. (2013) Long-term stabilization of high power optical parametric chirped-pulse amplifiers. Opt Express 21: 28987-28999.
23. Puppin M, Deng Y, Prochnow O, Ahrens J, Binhammer T, et al. (2015) 500 kHz OPCPA delivering tunable sub-20 fs pulses with 15 W average power based on an all-ytterbium laser. Opt Express 23: 1491-1497.
24. Riedel R, Stephanides A, Prandolini MJ, Gronloh B, Jungbluth B, et al. (2014) Power scaling of supercontinuum seeded megahertz-repetition rate optical parametric chirped pulse amplifiers. Opt Lett 39: 1422-1424.
25. Agrawal GP (2012) Nonlinear Fiber Optics Academic Press.
26. Smith AV, Do BT (2008) Bulk and surface laser damage of silica by picosecond and nanosecond pulses at 1064 nm. Appl Opt 47: 4812-4832.
27. Smith AV, Do BT, Hadley GR, Farrow RL (2009). Optical damage limits to pulse energy from fibers. IEEE J Sel Topics Quantum Electron 15: 153-158.
28. Dombi P, Racz P, Veisz L, Baum P (2014) Conversion of chirp in fiber compression. Opt Lett 39: 2232-2235.
29. Kim KS, Stolen RH, Reed WA, Quoi KW (1994) Measurement of the nonlinear index of silica-core and dispersion-shifted fibers. Opt Lett 19: 257-259.
30. Schneider W, Ryabov A, Lombosi C, Metzger T, Major Z, et al. (2014) 800-fs, 330- μJ pulses from a 100-W regenerative Yb:YAG thin-disk amplifier at 300 kHz and THz generation in LiNbO3. Opt Lett 39: 6604-6607.
31. http://www.nktphotonics.com/files/files/LMA-35-080926.pdf
32. Klenke A, Kienel M, Eidam T, Hadrich S, Limpert J, et al. (2013) Divided-pulse nonlinear compression. Opt Lett 38: 4593-4596.
33. Saraceno CJ, Heckl OH, Baer CRE, Sudmeyer T, Keller U (2011) Pulse compression of a high-power thin disk laser using rod-type fiber amplifiers. Opt Express 19: 1395-1407.
34. Fermann ME, Stock ML, Andrejco MJ, Silberberg Y (1993) Passive mode locking by using nonlinear polarization evolution in a polarization maintaining erbium-doped fiber. Opt Lett 18: 894-896.
35. Nodop D, Jauregui C, Schimpf D, Limpert J, Tunnermann A (2009) Efficient high-power generation of visible and mid-infrared light by degenerate four-wave-mixing in a large-mode-area photonic-crystal fiber. Opt Lett 34: 3499-3501.
36. Couairon A, Sudrie L, Franco M, Prade B, Mysyrowicz A (2005) Filamentation and damage in fused silica induced by tightly focused femtosecond laser pulses. Phys Rev B 71: 125435.
37. Osellame R, Chiodo N, Maselli V, Yin A, Zavelani-Rossi M, et al. (2005) Optical properties of waveguides written by a 26 MHz stretched cavity Ti: sapphire femtosecond oscillator. Opt Express 13: 612-620.